

ARTICLE

Open Access



Enhanced antibacterial properties of enteric glial cells attenuate intestinal inflammation through the GABA_BR-mediated autophagy pathway

Ziteng Deng¹, Jing Lan¹, Jiaqi Wang¹, Lu Wang¹, Zhihui Hao¹ and Yunfei Ma^{1*} 

Abstract

Enterotoxigenic *Escherichia coli* (ETEC) infection is a severe threat to global public health because of its high morbidity and mortality among children and infants. Enteric glial cells (EGCs) are involved in host–bacteria communication. However, the mechanisms through which EGCs interact with ETEC remain unclear. We attempted to assess whether γ -aminobutyric acid type B receptor (GABA_BR) activation participated in EGC autophagy during *Escherichia coli* K88 (ETECK88) infection. Alterations in autophagy and EGC activity were observed in the intestines of the ETECK88-infected mice, and similar results were obtained from experiments in which the EGCs were directly infected with ETECK88. EGC pretreatment with specific autophagy agonists significantly decreased the inflammatory response and bacterial burden, whereas pretreatment with inhibitors had the opposite effect. Interestingly, in EGCs, GABA_BR activation notably increased Beclin 1 and LC3 levels and autophagosome and autolysosome numbers, thus promoting autophagy activation and enhancing antimicrobial responses against ETECK88 infection. Furthermore, GABA_BR defense was mediated via myeloid differentiation factor 88 (MyD88) signaling in EGCs, which was proven to be based on the inhibition or overexpression of MyD88. Notably, comparable results of GABA_BR activation *in vivo* were observed in response to ETECK88, implicating this as a defense mechanism that reinforced antibacterial activity to alleviate intestinal inflammation in mice. Our study revealed previously unappreciated roles for GABA_BR in linking EGC antibacterial autophagy to strengthen host defense against ETECK88 infection, thus identifying GABA_BR as an important target for the treatment of infective enteritis.

Keywords *Escherichia coli* K88, Enteric glial cells, GABA_BR, Autophagy, MyD88

Background

Enterotoxigenic *Escherichia coli* (ETEC) strains are gram-negative pathogens that mainly colonize the host gastrointestinal tract (GI), representing a major public health threat worldwide by causing diarrhea in humans

and animals, thus resulting in enormous economic losses to society [1, 2]. ETEC virulence is intricately linked to the production of colonization factors and one or more enterotoxins [3]. An ever-growing body of research indicates that intestinal cells employ diverse defensive tactics to ward off microbial invaders [4]. These defense mechanisms include rapid epithelial cell turnover, preservation of the integrity of the epithelial barrier, elimination of infected cells, and autophagy [4]. In autophagy, cytosolic proteins are sequestered within double-membrane autophagosomes and are destined for degradation within

*Correspondence:

Yunfei Ma

yunfeima@cau.edu.cn

¹ State Key Laboratory of Veterinary Public Health and Safety, College of Veterinary Medicine, China Agricultural University, Beijing, China



© The Author(s) 2024. **Open Access** This article is licensed under a Creative Commons Attribution 4.0 International License, which permits use, sharing, adaptation, distribution and reproduction in any medium or format, as long as you give appropriate credit to the original author(s) and the source, provide a link to the Creative Commons licence, and indicate if changes were made. The images or other third party material in this article are included in the article's Creative Commons licence, unless indicated otherwise in a credit line to the material. If material is not included in the article's Creative Commons licence and your intended use is not permitted by statutory regulation or exceeds the permitted use, you will need to obtain permission directly from the copyright holder. To view a copy of this licence, visit <http://creativecommons.org/licenses/by/4.0/>.

lysosomes [5, 6]. This process is crucial for cell survival, especially during nutritional deprivation and microbial attacks. While moderate autophagy promotes cell survival, excessive autophagy can result in autophagic cell death. Notably, ETEC infection stimulates autophagy, and impeding this process reduces the survival rate of intestinal cells infected with ETEC [7]. However, the precise mechanism by which ETEC induces autophagy in intestinal cells and the exact role of autophagy during the onset of ETEC infection remain topics of ongoing debate.

It is now believed that the GI tract is a major entrance between the external environment and the internal body, serving as the primary defense against microorganisms and playing essential roles in preserving intestinal homeostasis by distinguishing between detrimental and beneficial bacteria [8–10]. Thus, guaranteeing that the intestinal environment performs well-organized host-bacteria communication and complicated interactions between the microbiota, immune system, enteric nervous system (ENS), and diverse cell types native to the lamina propria is extremely important [11–14]. Two vital cell types are present in the ENS: enteric neurons and enteric glial cells (EGCs), the latter of which are considered astrocyte-like neuroglia that express the glial fibrillary acidic protein (GFAP) and calcium-binding protein S100 β [15–17]. Recent evidence indicates that EGCs are tightly connected with enteric neurons and their processes, favoring several reflexes, such as gut motility and secretory function [18]. Moreover, EGCs also participate in the development and progression of various diseases, including inflammation, cancer, and infection, in which EGCs transform into pro- or anti-inflammatory phenotypes [16, 19]. In these situations, both the disappearance and increase in glial function contribute to intestinal homeostasis and alterations in GI pathophysiology. Previous data have shown that EGC autophagy is provoked in response to proinflammatory stimuli and activates antigen presentation [20]. The EGC-derived mediator GSNO relieves intestinal epithelial barrier (IEB) damage and inflammation caused by *Shigella flexneri* [21]. Thus, an emerging view from initial evidence is that EGCs may prevent the host from invading pathogens, which is likely beneficial for intercourse between the host and bacteria. However, few advanced reports on whether EGCs interact directly with pathogens exist.

Alterations in the levels of neurotransmitters from the ENS are involved in intestinal illness, and the secretion of neurotransmitters such as γ -aminobutyric acid (GABA) within the ENS could reveal innovative therapeutic targets for treating GI disorders [22–24]. In mammals, high concentrations of GABA are mainly observed in brain tissue, where it inhibits neurotransmission in the central nervous system (CNS) through two critical types

of receptors, GABA_A receptor (GABA_AR) and GABA_B receptor (GABA_BR) [25]. GABA_AR is an integral membrane ion channel complex that includes five subunits in which a minimum of 19 possible subunits are accessible for assembly, while GABA_BR is a G protein-coupled receptor composed of GABA_BR1 and GABA_BR2 subunits [26, 27]. Previous studies have suggested the potential of the administration of GABA or GABAergic (agonistic) drugs as novel treatments for inflammatory diseases and pathogenic infections [28–30]. However, those data mainly focused on GABA_AR rather than GABA_BR. Many of the effects of GABA involve GABA_BR in the brain, but there are few data regarding the regulatory function of GABA_BR in the intestine, especially during inflammation and bacterial challenge. Of special interest is the role of GABA_BR in the development, proliferation, and migration of colon cancer cells [26, 31]. Pretreatment with the GABA_BR agonist baclofen significantly inhibited malignant tumors of the colon via cAMP-dependent signaling [32]. Our previous research revealed that both GABA_BR subunits are expressed in EGCs and are required for normal pathophysiology. Whether alterations in GABA_BR signaling during microbial infection play a role in the molecular basis of antibacterial activity is unknown.

The goals of this study were to investigate the ability of EGCs to interact directly with ETECK88 and to explore the underlying mechanisms of GABA_BR in the antimicrobial function of EGCs. Our findings could reveal effective antimicrobial effects of EGCs and provide novel targets and important biological foundations for the treatment of gastrointestinal infections in humans and animals.

Results

ETECK88 reshapes autophagy and EGC activity in the mouse intestine

ETECK88 was used to induce experimental intestinal inflammation in C57BL/6 mice (Supplementary Fig. 1A), and the results showed that challenge with ETECK88 markedly impaired the jejunum and ileum tissues, as evidenced by body weight loss, severe damage to the epithelial layer, and increased expression of the proinflammatory factors IL-1 β , IL-6, and TNF- α (Supplementary Fig. 1B–F). To visualize bacterial colonization, a strain of ETECK88 with the mCherry gene that expressed red fluorescence was generated, and at 48 h postinfection, ETECK88-mCherry significantly colonized the jejunum and ileum contents of the mice (Supplementary Fig. 1G, H). Furthermore, a small portion of the ETECK88-mCherry group traveled from the site of implantation to the jejunum and ileum mucous layer, suggesting that ETECK88-mCherry was accessible to cells located in the intestinal mucosa (Supplementary Fig. 2). Autophagy is a well-recognized mechanism for targeting damaged

components or intracellular pathogens [5, 33], but unfortunately, ETECK88 infection obviously inhibited autophagy, as determined by Beclin 1 expression in jejunum and ileum tissues (Supplementary Fig. 3A, C). We validated that EGCs participate in defending against harmful substances and regulating inflammation [34]. Interestingly, the expression of GFAP, a reactive biomarker of EGCs, was markedly elevated in the jejunum and ileum of the ETECK88-infected mice (Supplementary Fig. 3B, D). These observations were reinforced by immunofluorescence analysis of the myenteric plexus of the jejunum and ileum, which revealed an increased number of GFAP- or S100 β -positive cells (Supplementary Fig. 3E–G). Prompted by these data, we investigated whether an increase in the number of mucosal glia occurred and found that ETECK88 significantly increased the number of EGCs in the mucosa of the jejunum and ileum, indicating that EGCs directly interact with ETECK88 (Supplementary Fig. 3H, I). These data suggest that ETECK88 opposes autophagy activation and alters EGC activity.

ETECK88 infection restrains autophagy in EGCs

To assess whether EGCs are directly involved in the regulation of host–bacteria interactions, cells were exposed to ETECK88 at MOIs of 5, 10, and 20 for 3, 6, and 12 h. The IL-6 mRNA level constantly increased with increasing infection time, but the dissolution or death of many of the cells occurred at 12 h (Supplementary Fig. 4A). Thus, we chose to expose EGC to an appropriate bacterial charge at an MOI of 10 for 3 and 6 h to minimize cell mortality. Surprisingly, confocal microscopy confirmed that ETECK88 was invasive, with intracellular ETECK88-mCherry observed in nearly all of the infected cells (Supplementary Fig. 4B). Moreover, gentamicin assays were used to eliminate extracellular bacteria (Supplementary Fig. 4C). To better understand the host pathways affected by ETECK88 subversion, we analyzed the autophagy system. Notably, the mRNA and protein levels of Beclin 1 and LC3 gradually decreased in a time-dependent manner upon ETECK88 exposure, which indicated that autophagic flux was blocked (Supplementary Fig. 4D–G). To further validate the autophagic flux status, we transfected cells with the pCMV-mCherry-GFP-LC3B plasmid, which is a fluorescently labeled protein tailor-made for autophagy research. Compared with mCherry, a vibrant red fluorescent protein, and GFP, a striking green fluorescent protein, both proteins are easily discernible under a fluorescence microscope. LC3 manifests in two distinct forms: LC3-I, which remains unbound in the cytoplasm, and LC3-II, which binds to the autophagosome membrane. pCMV-mCherry-GFP-LC3B is a fusion protein that integrates mCherry, GFP, and LC3.

As autophagy initiates within a cell, LC3-I transitions to LC3-II and attaches to the autophagosome membrane, resulting in yellow fluorescence emission from the cell, signifying the convergence of red and green fluorescent signals. Subsequently, as autophagosomes merge with lysosomes to form autophagolysosomes, the acidic environment causes GFP, which is sensitive to such conditions, to progressively lose its fluorescence, while mCherry maintains its bright red fluorescence, which is impervious to the acidic milieu. Hence, autophagolysosomes are exclusively indicated by red fluorescence. Autophagic flux is strengthened when both yellow and red puncta are increased in EGCs, whereas EGCs show decreases in both yellow and red puncta or when only yellow puncta are increased without red puncta changes, suggesting autophagic flux inhibition. Infection of EGCs with ETECK88, which is a wild-type strain devoid of fluorescein and thus does not emit any fluorescence, markedly reduced the number of yellow and red puncta in a time-dependent manner, suggesting the contraction of autophagosomes and the formation of autolysosomes (Supplementary Fig. 4H–J). Autophagy both targets and protects against a variety of intracellular bacterial pathogens, such as by establishing a bacteria-LC3B puncta complex. To further clarify this phenomenon, EGCs were transfected with pEGFP-LC3B for 24 h and then subjected to ETECK88-mCherry invasion. Regrettably, even in the presence of high levels of ETECK88-mCherry, there was very little formation of the bacteria-LC3B puncta mixture as autophagy was inhibited (Supplementary Fig. 4K). These data revealed that the resistance of EGCs to ETECK88 infection is disrupted as autophagy declines.

Activation of autophagy boosts EGCs against ETECK88 invasion

To explore whether autophagy is involved in host defense against microbial infection, EGCs were treated with RAPA, an agonist of autophagy; 3-MA, an inhibitor of autophagy that blocks autophagosome formation; or CQ, a specific late-phase autophagy inhibitor that restrains autophagic flux by impeding lysosomal degradation and obstructing autophagosome-lysosome fusion (Supplementary Fig. 5A–E). RAPA (10 μ M) for 3 h and 10 mM 3-MA and 25 μ M CQ for 1 h were chosen as the optimal concentration and treatment time for further investigation. After transfection with pCMV-mCherry-GFP-LC3B, EGCs exposed to RAPA exhibited a significant increase in yellow and green fluorescence in response to ETECK88, indicating an increase in the number of autophagosomes and autolysosomes. In contrast, the administration of 3-MA resulted in a substantial decrease in the number of LC3B puncta, whereas

CQ led to an increase in the number of LC3B puncta (Supplementary Fig. 5F–I). This phenomenon provided evidence that the autophagic flux of EGCs was retarded throughout the entire process after infection with ETECK88. Given that cytokines play critical roles during bacterial challenge, we further detected the expression of these factors through quantitative real-time PCR (qRT-PCR). The mRNA levels of IL-1 β and IL-6 were strongly decreased in the EGCs subjected to ETECK88 subversion after pretreatment with RAPA, while in sharp contrast, the TGF- β level was significantly increased (Fig. 1A–C). However, these changes were obviously reversed by treatment with 3-MA or CQ, suggesting that autophagy may be connected to the alleviation of inflammation. Interestingly, the formation of LC3B puncta and the extent of their colocalization with bacterial phagosomes were greatly greater in RAPA-treated/ETECK88-mCherry-infected EGCs than in untreated/ETECK88-mCherry-infected EGCs, which illustrated the possible effectiveness of autophagy in combating bacteria in EGCs (Fig. 1D, E). To further analyze the role of autophagy in bacterial killing, we examined the intracellular viability of the ETECK88 strains following the activation or inhibition of autophagy. As expected, RAPA significantly decreased the number of CFUs of ETECK88 in EGCs; however, 3-MA or CQ treatment significantly limited this effect (Fig. 1F, G). The data mentioned above support that the activation of autophagy triggers the antibacterial property of EGCs in the face of ETECK88 challenge.

GABA_BR activation promotes autophagy against ETECK88 infection in EGCs

Compared with extensive studies in the brain, few studies have illuminated the specific mechanism of GABA_BR in the intestine during the period of infection with pathogens. Previous research from our team revealed that GABA_BR in EGCs was involved in the pathway of bacterial invasion [34]. Therefore, we surmised that GABA_BR signaling may be connected with autophagy to enhance host defense by ETECK88. To test this hypothesis, we first detected the expression of GABA_BR in the intestinal tissues of mice upon ETECK88 challenge. The results showed that ETECK88 notably caused a reduction in GABA_BR protein levels in the jejunum and ileum (Fig. 2A). In line with these findings, qRT-PCR and Western blotting (WB) analysis revealed that the GABA_BR mRNA and protein levels decreased in a time-dependent manner in EGCs following ETECK88 infection, whereas the mRNA levels of the GABA_AR subunits did not change markedly with increasing infection time (Fig. 2B–D; Supplementary Fig. 6A, B). These data demonstrated that the subunits of GABA_BR were modulated by ETECK88

infection. To explore whether GABA_BR activation amplified the host defense against microbial infection, EGCs were treated with the GABA_BR agonist baclofen and then infected with ETECK88. Baclofen treatment led to significant inhibition of IL-6 and an increase in TGF- β in EGCs during ETECK88 infection, indicating an anti-inflammatory effect on GABA_BR signaling during pathogen challenge (Fig. 2E, F). We next investigated whether autophagy is involved in GABA_BR activation to trigger antimicrobial effects during intracellular bacterial infection. In particular, genes associated with autophagy, including Beclin 1 and LC3, were substantially upregulated at the mRNA or protein level in baclofen-treated cells, demonstrating that GABA_BR elicitation induced the activation of autophagy (Fig. 2G–J). We used a tandem-LC3 vector (pCMV-mCherry-GFP-LC3B) to confirm that baclofen stimulated bona fide autophagic flux, as evidenced by the marked increase in yellow and red fluorescence within EGCs, suggesting an increase in the number of autophagosomes and autolysosomes (Fig. 2K–M). We thus explored whether GABA_BR-induced autophagy activation was required for the phagocytosis process during ETECK88-mCherry invasion. The number of LC3B puncta and the extent of their colocalization with ETECK88-mCherry phagosomes were significantly elevated in the infected cells (Fig. 2N). Importantly, lower bacterial burdens were observed in the baclofen-treated cells following ETECK88 invasion (Fig. 2O, P; Supplementary Fig. 6C, D). These results demonstrate that GABA_BR signaling contributes to protecting the host from ETECK88 infection through the activation of autophagy.

MyD88 is essential for GABA_BR-mediated autophagy activation in EGCs challenged with ETECK88

We further examined the mechanism by which GABA_BR activated autophagy *in vitro* and *in vivo*. MyD88 has been reported to act as a major adaptor molecule downstream of several surface and cytosolic pattern recognition receptors [35, 36]. MyD88-dependent autophagy inhibition contributes to intestinal inflammation damage [37]. Our results revealed that compared with uninfected mice, ETECK88-infected mice had significantly greater levels of the MyD88 protein in the jejunum and ileum (Supplementary Fig. 7A, B). MyD88 is necessary for responses to Toll-like receptors (TLRs), the stimulation of which leads to the expression of a wide range of genes involved in innate and adaptive immunity against pathogens [38–40]. Remarkably, infection of EGCs with ETECK88 significantly decreased the mRNA levels of TLR1, TLR3, TLR4, TLR6, and TLR9 in a time-dependent manner, but not those of TLR5 (Supplementary Fig. 7C–J). In contrast, in line with the *in vivo* data, both the mRNA and

protein levels of MyD88 in EGCs were upregulated following ETECK88 invasion, while ETECK88 seemed to have little impact on the mRNA secretion of NF- κ B pathway-related genes (Supplementary Fig. 7K–Q). These data were consistent with our hypothesis that MyD88 is likely the major molecule involved in GABA_BR-mediated autophagy activation in response to ETECK88 challenge.

We thus examined the effects of baclofen on the expression of TLRs and MyD88 in EGCs during infection. Intriguingly, GABA_BR activation increased the levels of mRNAs encoding TLR3, TLR4, TLR6, and TLR9 but not MyD88, which was significantly impeded at both the mRNA and protein levels, in ETECK88-infected EGCs (Fig. 3A–C; Supplementary Fig. 8A–D). We next sought to investigate the effects of MyD88 on the ETECK88-mediated reduction in autophagy in EGCs. We performed genetic silencing of MyD88 using a plasmid system (pLV3-U6-MyD88-shRNA-CopGFP-Puro), and WB confirmed that MyD88 protein expression was efficiently downregulated in EGCs, especially that of shRNA MyD88-1, which achieved improved expression (Supplementary Fig. 9A, B). As expected, in MyD88-silenced cells infected with ETECK88, the mRNA levels of the proinflammatory cytokines IL-1 β and IL-6 were markedly decreased, while the production of the anti-inflammatory factor TGF- β was increased (Fig. 3D–F). However, these changes were significantly reversed by MyD88 overexpression via the pLV3-CMV-MyD88 (rat)-3xFLAG-CopGFP-Puro plasmid (Supplementary Fig. 10A–C). Using a silencing plasmid to inhibit MyD88 expression, we showed that MyD88 inhibition strongly increased the expression of Beclin 1 and LC3 at the mRNA and protein levels, respectively, in cells challenged with ETECK88; nevertheless, MyD88 overexpression had the opposite effect (Fig. 3G–J; Supplementary Fig. 10D–G). ETECK88-induced autophagy inhibition in EGCs was closely linked to MyD88 signaling. Next, to monitor the effect of MyD88 inhibition on autophagic flux, we treated EGCs with various concentrations of the MyD88 inhibitor TJ-M2010-5 before ETECK88 infection and treated them with 5 μ M TJ-M2010-5 for further experiments (Supplementary Fig. 9C, D). Increased Beclin 1 protein production was also observed in EGCs challenged with

ETECK88 following exposure to TJ-M2010-5, which was consistent with the MyD88 silencing results (Supplementary Fig. 9E, F). In the autophagy flux assay, TJ-M2010-5 induced significant autophagosome and autolysosome accumulation in ETECK88-infected cells, which were characterized by mCherry and GFP (yellow) or mCherry (red) fluorescence signals, respectively (Fig. 3K–M). TJ-M2010-5 treatment markedly elevated the colocalization of ETECK88-mCherry phagosomes with autophagosomes, further confirming that MyD88 plays a critical role in autophagy-mediated antimicrobial activity (Fig. 3N). Additionally, the inhibitory effects of EGC-mediated silencing of MyD88 on the survival of ETECK88-treated cells were greater than those on the survival of untreated cells (Fig. 3O, P). These data strongly suggest that MyD88 is required for GABA_BR-induced autophagy enhancement and antimicrobial responses against ETECK88 infection.

Activation of GABA_BR could relieve enteritis by restraining the inflammatory response and inhibiting ETECK88 colonization

These data collectively show that GABA_BR activation is critical when host defenses are mounted against ETECK88 infection. We thus hypothesized that systemic GABA_BR triggers would decrease host susceptibility to such infection. Mice were intraperitoneally pretreated with 10 mg/kg baclofen for 7 days before and after infection (Fig. 4A). Next, the mice were infected with ETECK88. Interestingly, the administration of baclofen to the ETECK88-infected mice significantly ameliorated intestinal inflammation, as indicated by decreased diarrhea symptoms, body weight loss and spleen weight augmentation, as well as less disruption of the mucosal epithelium in the jejunum and ileum tissues (Fig. 4B–D; Supplementary Fig. 11A–C). Additionally, since goblet cells (GCs) that express mucin are present in the intestinal mucosal epithelium [41], we performed AB-PAS staining and revealed that ETECK88 resulted in massive loss of GCs in the villi of the jejunum and ileum, but fortunately, the GCs were increased after baclofen treatment (Fig. 4E). In addition, baclofen effectively improved the production of cytokines, including

(See figure on next page.)

Fig. 1 Autophagic activation promotes the antibacterial activity of EGCs against ETECK88 infection. **A–C** qRT-PCR analysis of IL-1 β , IL-6, and TGF- β mRNA expression. **D, E** Representative images showing the interaction between ETECK88-mCherry and autophagosomes. EGCs were transfected with the pEGFP-LC3B plasmid, and cells were pretreated with or without RAPA or RAPA plus 3-MA or CQ and then infected with or without ETECK88-mCherry for 3/6 h. The binding regions of bacteria and autophagosomes are denoted by white arrows. Scale bar, 20 μ m. **F, G** Intracellular survival of ETECK88-treated EGCs pretreated with or without RAPA or RAPA plus 3-MA or CQ. For qRT-PCR, GAPDH was used for normalization, and the mean fold changes compared to those in the CON group were calculated according to the $2^{-\Delta\Delta CT}$ method. The data are shown as the mean \pm SEM. * $p < 0.05$, ** $p < 0.01$, *** $p < 0.001$

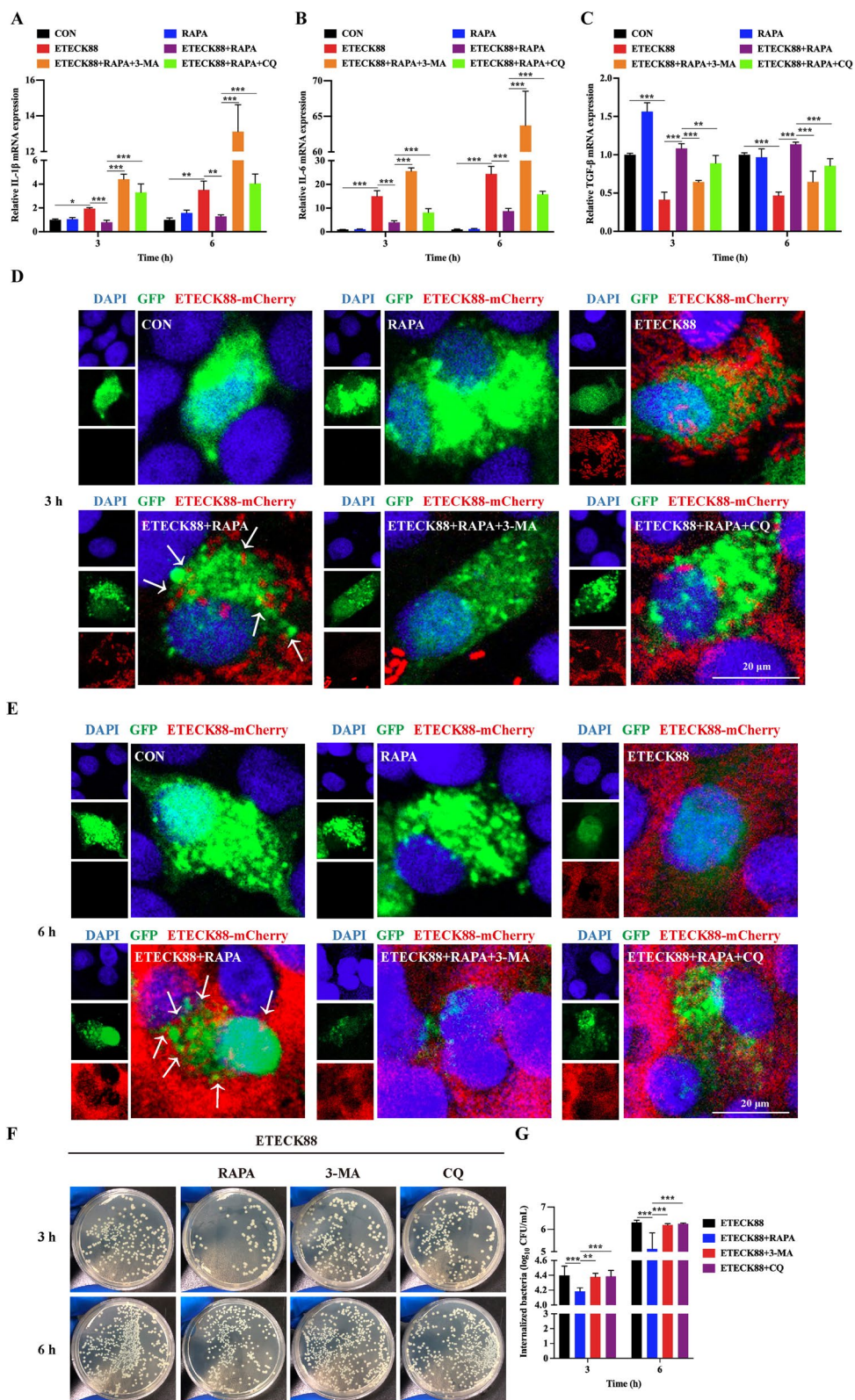


Fig. 1 (See legend on previous page.)

proinflammatory factors (IL-1 β , IL-6, IL-17A, TNF- α , and MCP-1), chemokines (CXCL9) and colony-stimulating factor (GM-CSF), in the jejunum and ileum tissues of ETECK88-infected mice and enhanced the production of anti-inflammatory factors (IL-4, IL-10, and TGF- β), indicating that GABA $_B$ R activation improved inflammatory responses (Fig. 4F–I). Immune cells such as macrophages, which are a significant source of inflammatory factors, are activated to respond to disadvantageous environmental stimuli, including pathogenic bacteria, when inflammation occurs [42]. We next detected the mRNA or protein levels of immune-related molecules, which are representative of M1/M2 macrophages, through qRT-PCR or WB. Our data showed that the mRNA or protein levels of M1 macrophage markers, including CD16, CD32, CD68, CD80, CD86, MHC II, and iNOS, in the jejunum and ileum of ETECK88-infected mice were significantly decreased following pretreatment with baclofen (Fig. 4J, K, N–P). Interestingly, we also observed that baclofen significantly increased the levels of genes encoding the M2 macrophage markers Arg1 and CD206, suggesting that GABA $_B$ R activation induced a state favoring an anti-inflammatory phenotype in the jejunum and ileum tissues (Fig. 4L, M).

To better understand the suppressive effects of GABA $_B$ R signaling on intestinal inflammation, we evaluated the ability of ETECK88 to colonize the enteric contents of mice. Intriguingly, ETECK88-mCherry growth in the jejunum and ileum was markedly restrained upon treatment with baclofen (Fig. 4Q, R). These findings suggested that GABA $_B$ R activation strongly adjusted the intestinal flora. Hence, to gain further insight into the effects of GABA $_B$ R activation on the microbiota in the gut, 16S rDNA sequencing of ileum contents was performed. Further validation via a CFU counting assay revealed that baclofen administration significantly reversed intestinal flora maladjustment in mice infected with ETECK88, as indicated by a decrease in the

abundance of harmful bacteria such as *Escherichia coli* and an increase in the abundance of *Bacteroides*, *Firmicutes*, and *Lactobacillus*, which have been characterized as probiotics (Fig. 4S, T; Supplementary Fig. 11D–G). The evidence above suggests that the activation of GABA $_B$ R in mice significantly compromises susceptibility to ETECK88.

GABA $_B$ R activation enhances host protection against ETECK88 infection through MyD88-mediated autophagy in the EGCs of mice

To further demonstrate the mechanisms underlying the protective effects of baclofen in ETECK88-infected mice, we first analyzed the TLR4/MyD88/NLRP3 signaling pathway. In the jejunum and ileum tissues of mice, ETECK88 increased both the mRNA and protein levels of TLR4, MyD88, and NLRP3, but this increase was successfully suppressed by pretreatment with baclofen (Fig. 5A–E). Dramatic autophagy activation dependent on MyD88 inhibition was demonstrated in an *in vitro* experiment in which EGCs were challenged with ETECK88. Notably, in the inflamed lesions of the jejunum and ileum, Beclin 1 and LC3 were downregulated at the mRNA and protein levels, respectively; to some extent, the administration of baclofen elevated these expression levels (Fig. 5F–I). These data corresponded with those of the *in vitro* experiments. Moreover, GABA $_B$ R activation notably impaired the expression of GFAP in the jejunum and ileum tissues of mice infected with ETECK88, which strongly verified the close relationship between GABA $_B$ R and EGCs in the antibacterial process (Fig. 5J, K). Consistent with the above data, as shown by immunofluorescence staining for GFAP (red) and S100 β (green), GABA $_B$ R activation was accompanied by a decrease in the number of EGCs in the myenteric plexus of the jejunum and ileum of ETECK88-infected mice (Fig. 5L–N). Within the mucosal layers of the intestine, EGCs immunolabeled

(See figure on next page.)

Fig. 2 GABA $_B$ R activation protects EGCs from ETECK88 invasion by enhancing autophagy. **A** ELISA was used to measure the levels of GABA $_B$ R in the intestines of the mice. **B** EGCs were subjected to qRT-PCR to determine the mRNA levels of GABA $_B$ R. **C, D** The levels of GABA $_B$ R in EGCs were analyzed by WB. **E–H** The mRNA expression levels of IL-6, TGF- β , Beclin 1, and LC3 in EGCs were assessed by qRT-PCR. Cells were treated with or without baclofen and then infected with or without ETECK88. **I, J** EGCs were pretreated with or without baclofen and then analyzed for Beclin 1 protein expression after ETEC infection. **K, L** Average number of autophagosomes (yellow) and autolysosomes (red) in each cell (>20 cells/group). **M** Transiently transfected EGCs expressing pCMV-mCherry-GFP-LC3B were treated with or without baclofen and then challenged with or without ETECK88. Confocal microscopic analysis of LC3B. Scale bar, 20 μ m. **N** Confocal microscopic analysis of the interaction between ETECK88-mCherry and autophagosomes. EGCs were transfected with the pEGFP-LC3B plasmid, and the cells were treated with or without baclofen and then infected with or without ETECK88-mCherry. The binding regions of bacteria and autophagosomes are denoted by white arrows. Scale bar, 20 μ m. **O, P** Intracellular survival of ETECK88-treated EGCs pretreated with or without baclofen. For qRT-PCR, GAPDH was used for normalization, and the mean fold changes compared to those in the CON group were calculated according to the $2^{-\Delta\Delta CT}$ method. For WB, expression levels were normalized to the expression of β -actin. The data are shown as the mean \pm SEM. * or # $p < 0.05$, ** or ## $p < 0.01$, *** or ### $p < 0.001$

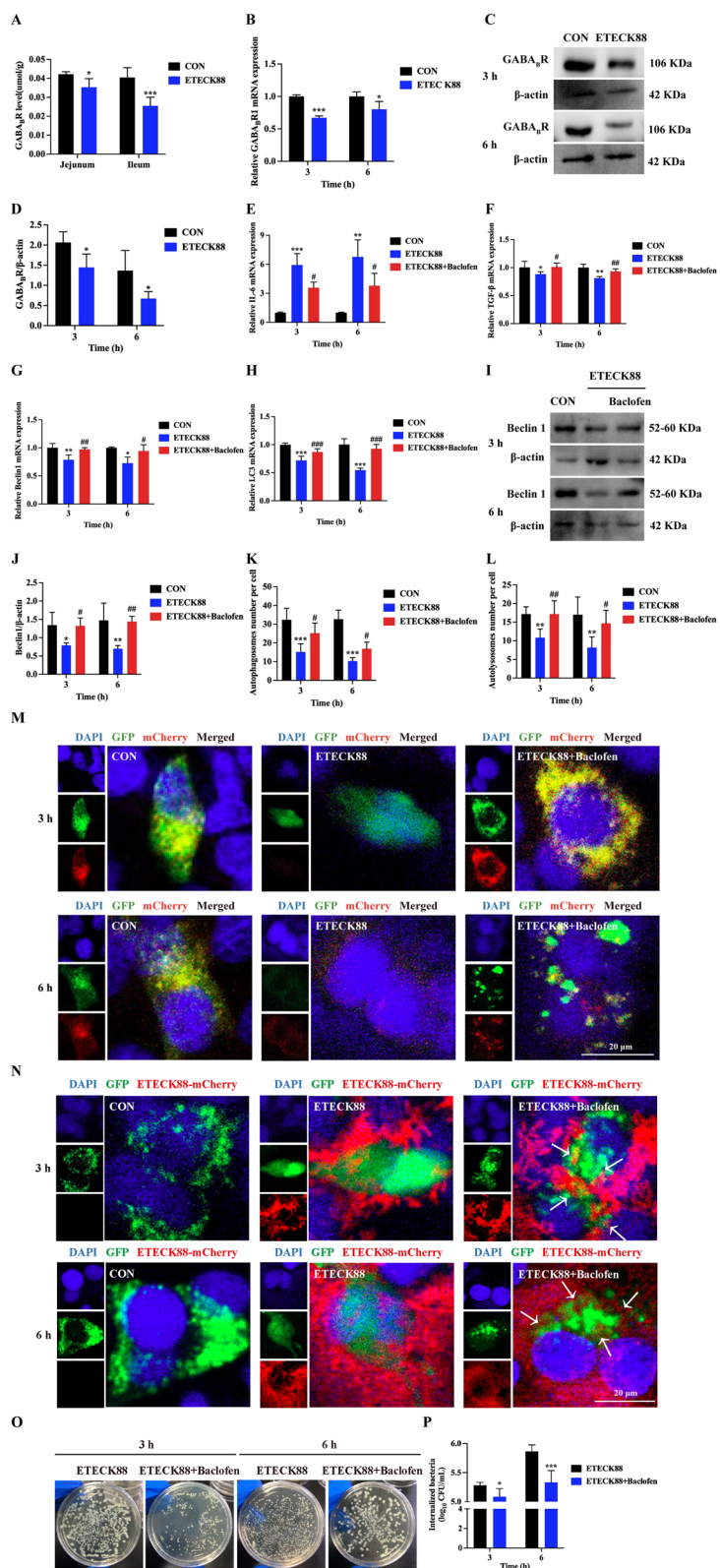


Fig. 2 (See legend on previous page.)

for GFAP and/or S100 β (green) were found to reside primarily in mice challenged with ETECK88, but baclofen administration significantly weakened these effects (Fig. 5O, P). Taken together, these results provide convincing evidence to support our emerging view that GABA $_B$ R activation inhibits MyD88 to strengthen EGC autophagy to enhance host defense.

Discussion

Our data showed that GABA $_B$ R activation reduced susceptibility to ETECK88 infection and thus contributed to antimicrobial host defenses both *in vitro* and *in vivo*. Compared with extensive reports in the brain, few studies have investigated the function of GABA $_B$ R signaling in the intestine, especially in the ENS, such as in EGCs. Herein, we concentrated on EGCs, which serve as immune cells to battle against intracellular bacterial infection, in the context of GABA $_B$ R host defense. Notably, the MyD88 inhibition-mediated increase in autophagy was closely involved in the GABA $_B$ R defense system of EGCs during infection (Fig. 6).

The gram-negative bacteria ETEC is frequently observed in the gastrointestinal microbiota [43]. ETECs are a group of pathogens that normally colonize the small intestine, where they generate and transport plasmid-encoded heat-labile and/or heat-stable enterotoxins [44]. In total, these conditions lead to tens of thousands of cases of diarrhea in humans and livestock annually. Consistent with the existing findings, our data showed that oral administration of ETECK88 seriously impaired the health of mice, with one of the most obvious changes observed in body weight. The villus plays a critical role in the small intestine and plays an essential role in eradicating harmful bacteria and acquiring nourishment [45]. Intestinal mucosa regression with epithelial exfoliation is commonly observed in ETECK88-infected piglets, as well as in mice challenged with ETECK88. Importantly, we found that at 48 h postinfection, a tremendous amount of

ETECK88-mCherry with red fluorescence colonized the jejunum and ileum contents. Considering the high degree of bacterial colonization, we surmised that ETECK88-mCherry would have a good chance of traveling from the contents to the mucous layer of the jejunum and ileum. The confocal microscopy results validated this claim, although only small amounts of ETECK88-mCherry were monitored. Thus, close contact between ETECK88 and cells located in intestinal tissues was observed.

An increasing number of studies have shown that EGCs are the primary contributors to the development and progression of GI disease, which provides insight into the role of EGCs in response to stimuli, cancer, and pathogenic bacteria [46]. *In vivo* and *in vitro* experiments revealed that EGC relieves the IEB injury and inflammation caused by *Shigella flexneri* through the expression of the key mediator GSNO [21]. EGCs are also activated by exogenous stimuli, such as LPS and IFN- γ , to secrete MHC II, iNOS and inflammatory factors to participate in the regulation of intestinal illness [47]. In the intestinal mucosa of patients with inflammatory bowel disease, the EGC network is abnormal, and the protein levels of particular EGC-derived markers, GFAP and S100 β , are high [48]. In the lesioned jejunum and ileum of ETECK88-infected mice, increased expression of GFAP was detected, which was further confirmed in the myenteric plexus through immunofluorescence. These findings suggested that the abnormal activity of EGCs was caused by ETECK88. It has been reported that abnormally and excessively proliferating EGCs can migrate from sites of the myenteric plexus to the intestinal mucous layer [16]. Consistently, by staining for GFAP and S100 β with a single fluorescence, we found that the number of EGCs in the intestinal mucosa was notably increased. In combination with the location of ETECK88 in the intestinal mucosa, there was a strong possibility that EGCs contacted ETECK88 directly.

(See figure on next page.)

Fig. 3 MyD88 inhibition decreases ETECK88 invasion in EGCs through the promotion of autophagy. **A** MyD88 expression was measured by qRT-PCR. The EGCs were treated with or without baclofen and then infected with or without ETECK88. **B, C** EGCs were treated with or without baclofen, followed by WB analysis to test the protein expression of Beclin 1 after ETECK88 infection. **D–H** MyD88 in EGCs was silenced, and the mRNA expression levels of IL-1 β , IL-6, TGF- β , Beclin 1, and LC3 were analyzed using qRT-PCR after ETECK88 infection. **I, J** EGCs with or without MyD88 silencing were infected with ETECK88, and then, WB was used to analyze the protein level of Beclin 1. **K, L** Autophagosomes (yellow) and autolysosomes (red) were counted from at least 20 random cells. **M** After pCMV-mCherry-GFP-LC3B transfection, EGCs were loaded with or without TJ-M2010-5 and then challenged with or without ETECK88. Confocal microscopic analysis of LC3B. Scale bar, 20 μ m. **N** EGCs were transfected with pEGFP-LC3B, exposed to TJ-M2010-5, and then infected with ETECK88-mCherry. The colocalization of ETECK88-mCherry and autophagosomes was examined by confocal microscopy. The binding regions of bacteria and autophagosomes are denoted by white arrows. Scale bar, 20 μ m. **O, P** EGCs were treated with or without shRNA against the MyD88 plasmid, after which the intracellular survival of ETECK88 was estimated. For qRT-PCR, GAPDH was used for normalization, and the mean fold changes compared to those in the CON group were calculated according to the $2^{-\Delta\Delta CT}$ method. For WB, expression levels were normalized to the expression of β -actin. The data are shown as the mean \pm SEM. ns - not significant, * or # $p < 0.05$, ** $p < 0.01$, *** $p < 0.001$

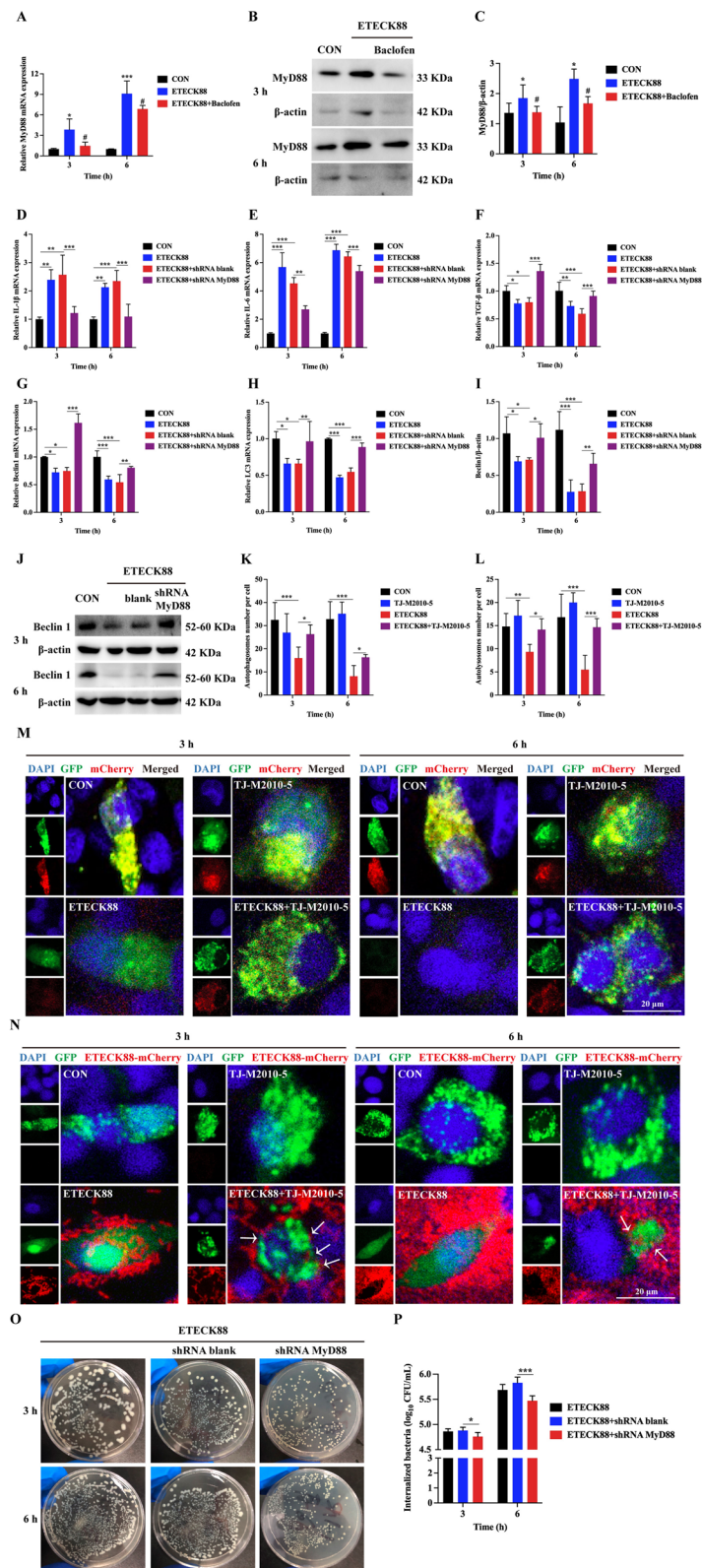


Fig. 3 (See legend on previous page.)

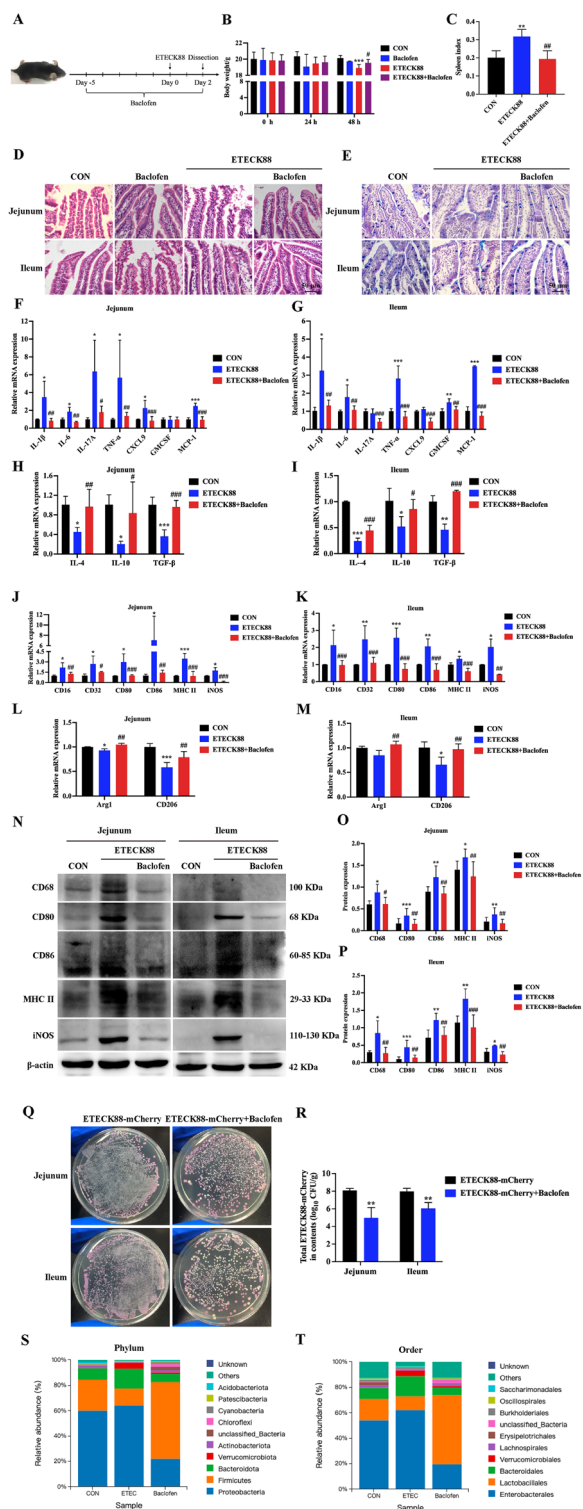


Fig. 4 GABA_BR activation alleviates ETECK88-induced intestinal damage *in vivo* through downregulating inflammation and bacterial colonization. **A** The protocol for treating ETECK88-treated mice with baclofen. **B** Quantification of body weight as a measure of intestinal inflammation severity in the different treatment groups. **C** The indices of the spleen. **D** Representative H&E-stained images of intestinal tissues. Scale bar, 50 μm. **E** AB-PAS staining of intestinal sections from the different treatment groups. Scale bar, 50 μm. **F–M** The mRNA expression levels of inflammatory factors and immune-related genes in the intestine were analyzed using qRT–PCR. **N–P** WB products of immune-related markers in intestinal tissues from the different groups. **Q, R** Intestinal content of ETECK88-mCherry in mice. **S, T** 16S rDNA sequencing results of the relative abundance of intestinal bacteria in mice at the phylum and order levels in each group. For qRT–PCR, GAPDH was used for normalization, and the mean fold changes compared to those in the CON group were calculated according to the 2^{-ΔΔCT} method. For WB, expression levels were normalized to the expression of β-actin. The data are shown as the mean ± SEM. * or # *p* < 0.05, ** or ## *p* < 0.01, *** or ### *p* < 0.001

We thus infected EGCs with ETECK88 directly *in vitro*. Delightedly, ETECK88 resulted in high expression of IL-6 mRNA during infection, suggesting that EGCs possess the ability to deal directly with ETECK88. We recently demonstrated that EGCs express the mRNAs and proteins of immune-related molecules, such as CD16, CD32, CD80, CD86, MHC II, iNOS, Arg1 and CD206, to act as immune cells, such as macrophages, involved in various physiological and pathological processes [34]. During infection, macrophages are crucial to the innate immune response to pathogens, and their fundamental role, antimicrobial activity, is to eliminate internalized bacteria [49]. In this event, as a housekeeper, autophagy sustains cellular homeostasis by killing intracellular bacteria through the formation of autophagolysosomes [50]. We found that ETECK88 significantly invaded EGCs, as determined by confocal microscopy and CFU counting assays. The elimination of autophagic substrates involves two essential steps: the initial recognition of degradation targets by autophagy mechanisms, followed by their transportation to autolysosomes for elimination. p62 plays a crucial bridging role between LC3B and ubiquitinated substrates destined for degradation [51, 52]. This adaptor protein binds to ubiquitinated proteins, integrates them into autophagosomes, and ultimately aids in their fusion with lysosomes, creating autolysosomes for efficient waste removal. When autophagy flux is disrupted, p62 levels increase, while activated

autophagy flux results in decreased p62 levels. In our study, we detected a substantial decrease in the expression of autophagy-related molecules, specifically Beclin 1 and LC3, accompanied by a reduction in the number of autophagosomes and autolysosomes upon infection of EGCs with ETECK88. These observations suggest that autophagy is suppressed, indicating a potential increase in p62 protein levels during this phase. This further suggested a notable decrease in the antibacterial activity of EGCs. We thus first investigated the role of autophagy in protecting EGCs from intracellular bacteria. Interestingly, the activation of autophagy by RAPA obviously inhibited the intracellular survival of ETECK88, while 3-MA or CQ had the opposite effect, demonstrating that the enhancement of EGC autophagy has antimicrobial effects. Moreover, autophagy activation could also improve the inflammatory response, as indicated by decreased levels of IL-1 β and IL-6 and increased expression of TGF- β , suggesting that autophagy is closely linked to inflammation during ETECK88 infection.

Recent results on the GABAergic activation of antibacterial capacity in macrophages and *in vivo* evidence revealed the critical role of GABA_AR in innate immune responses to intracellular pathogen challenge [28]. These results revealed that the increase in autophagy was induced by GABA or GABA_AR activation in macrophages and thus contributed to phagosomal maturation and the host defense capacity against invasive bacteria. Our previous report strongly indicated that GABA_BR rather than GABA_AR in EGCs participates in the modulation of the bacterial invasion pathway of epithelial cells [34]. However, the functions of GABA_BR in EGCs, especially in the modulation of autophagy during bacterial invasion, are still not well known. Surprisingly, in the present study, ETECK88 resulted in lower levels of GABA_BR both in intestinal tissues and EGCs, indicating that GABA_BR signaling was inhibited following bacterial infection. Although the levels of GABA_AR subunits, including GABA_AR θ and GABA_AR ρ 3, were changed at 3 h postinfection, their expression did not seem to change much at 6 h. Therefore, we mainly assessed the effects of GABA_BR activation on the elicitation of host defense away from

ETECK88 invasion. The application of baclofen notably reduced the expression of inflammatory factors in EGCs infected with ETECK88, thus highlighting the anti-inflammatory effects associated with GABA_BR activation. Furthermore, through the use of baclofen, the activation of GABA_BR significantly augmented the expression of Beclin 1 and LC3, which was paralleled by an increase in the number of autophagosomes and autolysosomes, ultimately resulting in autophagy enhancement. Concurrently, p62 protein levels within EGCs decreased. The amplification of autophagy in turn promoted the binding of autophagosomes to ETECK88. By using a CFU assay to determine the intracellular survival of ETECK88, the ability of EGCs to scavenge invasive bacteria was determined. In this study, we primarily employed baclofen, a lipophilic derivative of γ -aminobutyric acid (GABA), which functions as an orally effective and highly selective agonist of GABA_BR. Baclofen is widely recognized as a highly effective agonist for activating GABA_BR, and it has been successfully commercialized and employed in clinical practice. It is possible that baclofen treatment does not notably alter the expression levels of GABA_BR but may instead affect the molecular conformation of the receptor, which represents the activation of GABA_BR [53]. However, currently, there is no definitive marker available to accurately demonstrate the activation of GABA_BR by baclofen. Previous studies have demonstrated that by mimicking the actions of GABA, baclofen triggers slow presynaptic inhibition via the activation of GABA_BR in various brain cells, such as neurons, astrocytes, microglia, and oligodendrocytes [53–58]. In this study, our main focus was not to observe changes in GABA_BR expression following baclofen treatment but to explore the specific functions of the activated GABA_BR. Our previous studies demonstrated that upon GABA_BR activation, baclofen significantly modulates the phenotypic polarization of EGCs, suppresses the expression of proinflammatory cytokines, and elevates the levels of anti-inflammatory factors, ultimately mitigating LPS-induced inflammation [34]. Based on these analyses and our findings, we believe that baclofen obviously activated the GABA_BR in the present study.

(See figure on next page.)

Fig. 5 Activation of GABA_BR linked to EGC autophagy protects mice from ETECK88 infection by inhibiting MyD88. **A, B** qPCR analysis of TLR4, MyD88, and NLRP3 mRNA levels in the intestinal tissues of mice. **C–E** Representative images of TLR4, MyD88, and NLRP3 protein levels in the intestinal tissues of mice. **F, G** qPCR analysis of Beclin 1 and LC3 mRNA levels in the intestines of mice in different groups. **H–K** The protein expression levels of Beclin 1 and GFAP in mouse intestinal tissues were detected by WB analysis. **L–N** Representative images showing GFAP (red) and S100 β (green) in the myenteric plexus of the mouse intestine. Scale bar, 20 μ m. **O, P** Total EGCs in the intestinal mucosa of mice were marked by single immunofluorescence staining for GFAP and/or S100 β (green). Positive locations are denoted by white arrows. Scale bar, 20 μ m. For qRT-PCR, GAPDH was used for normalization, and the mean fold changes compared to those in the CON group were calculated according to the $2^{-\Delta\Delta CT}$ method. For WB, expression levels were normalized to the expression of β -actin. The data are shown as the mean \pm SEM. * or # $p < 0.05$, ** or ## $p < 0.01$, *** or ### $p < 0.001$

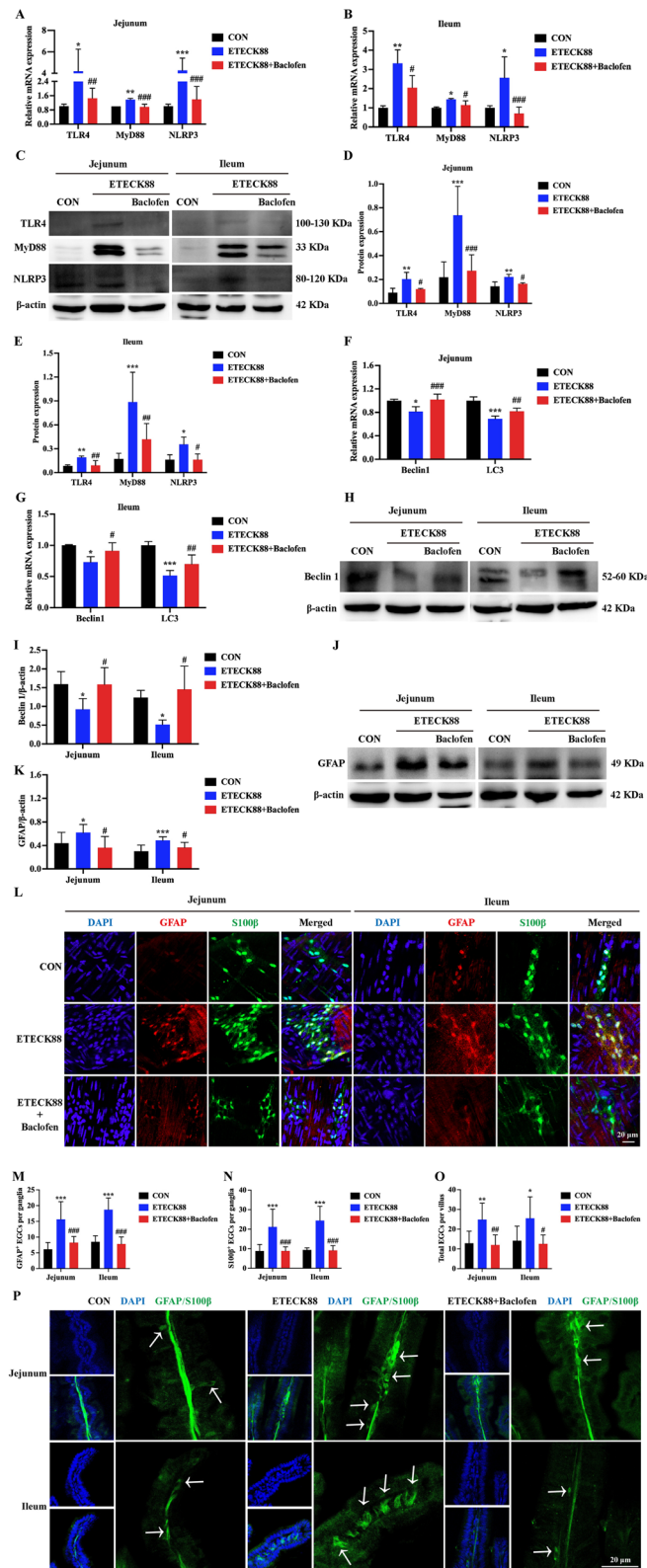


Fig. 5 (See legend on previous page.)

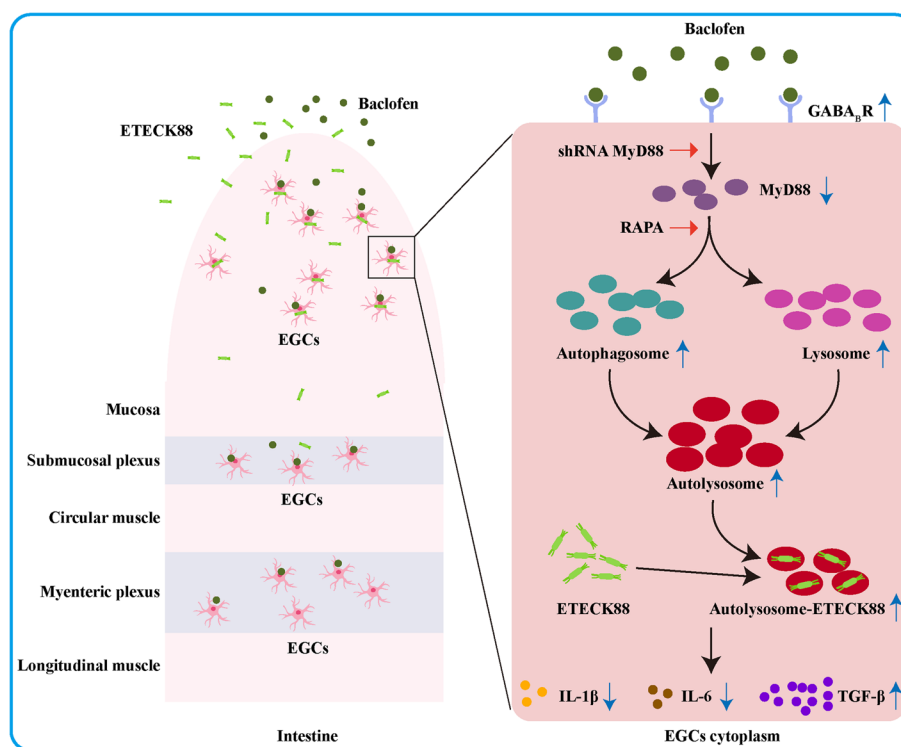


Fig. 6 Proposed model for GABA_BR activation accelerating autophagy formation by inhibiting MyD88 signaling to strengthen EGC antibacterial activity. Pretreatment of EGCs with the GABA_BR agonist baclofen significantly decreased MyD88 levels upon infection with ETECK88. Over time, the number of autophagosomes and lysosomes increased, and the number of autolysosomes and the extent of their colocalization with ETECK88 were obviously elevated in the infected cells. Importantly, the levels of the proinflammatory factors IL-1 β and IL-6 decreased, while the production of the anti-inflammatory mediator TGF- β increased. Hence, the antibacterial function of EGCs was ultimately reinforced

Several studies in mice and humans have demonstrated that in the brain, innate immunity is mainly manipulated by TLRs, which are primarily expressed on astrocytes and microglia [59]. In a common state, astrocytes show almost no expression of TLRs; however, their secretion is increased promptly following microbial infection [59]. It has been reported that EGCs share analogous roles with astrocytes, which are located mainly in the CNS and exhibit similar morphology and functions. On this basis, EGCs express TLRs at very low levels, indicating that EGCs have the capacity to respond to exogenous stimuli and pathogen challenge and thus elicit innate immunity in the intestine [59]. In agreement with these findings, TLRs were detectable in the EGC line. However, the expression of TLR1, TLR3, TLR4, TLR6, and TLR9, but not that of TLR5, decreased following ETECK88 infection. The decrease in TLR levels in EGCs may be a self-protective mechanism during the inflammatory damage caused by ETECK88. However, GABA_BR activation significantly boosted the mRNA production of TLRs, suggesting that GABA_BR signaling participates in self-protective mechanisms and innate immunity in EGCs. When microbial

invasion occurs, TLRs play a role in recognizing pathogen-associated molecular patterns through MyD88-dependent and MyD88-independent signaling [60]. As a vital adaptor for TLRs other than TLR3, activated MyD88 stimulates downstream pathways such as the NF- κ B signaling pathway, which is associated with inflammation and bacterial infection [61]. In contrast to those of TLRs, our data revealed that both the mRNA and protein levels of MyD88 in intestinal tissues and EGCs were elevated following ETECK88 infection. Although high expression of cytokines was found in EGCs upon ETECK88 infection, activated MyD88 did not seem to affect the NF- κ B pathway, which is considered the most effective signaling pathway for inflammatory factor production. Therefore, MyD88 may be directly involved in the regulation of ETECK88. Increasing amounts of data have demonstrated that MyD88 is significant for infection-pathogen elimination both *in vivo* and *in vitro* [62]. For example, mice in which the MyD88 gene was knocked out were more sensitive to *Staphylococcus aureus* [60]. We showed that GABA_BR-mediated autophagy in EGCs effectively inhibited intracellular ETECK88. Owing to

these findings, we hypothesized that MyD88 likely participates in the GABA_BR-autophagy pathway. As expected, GABA_BR activation greatly decreased the expression of MyD88 in mouse intestinal tissues and EGCs. Intriguingly, our *in vitro* data revealed that suppressing MyD88 via either a shRNA-MyD88 plasmid or a TJ-M2010-5 inhibitor significantly reduced the proinflammatory cytokines IL-1 β and IL-6 while simultaneously increasing TGF- β levels. This cytokine shift implies that inhibiting MyD88 could alleviate inflammation, offering therapeutic advantages. When MyD88 was inhibited using inhibitors or shRNA-MyD88 plasmids, we observed a marked increase in the expression of Beclin 1 and LC3, along with an increase in the number of autophagosomes and autolysosomes. These observations suggest enhanced autophagy in EGCs infected with ETECK88. Additionally, we assumed a possible decrease in p62 protein levels. Moreover, there was a noticeable increase in the number of autolysosomes associated with ETECK88, accompanied by a decrease in the number of bacterial colonies on the plate. This indicates that MyD88 inhibition is effective in scavenging and countering ETECK88 invasion. Overall, our findings unequivocally demonstrate that the activation of GABA_BR promotes autophagy enhancement and inflammation reduction in EGCs through the MyD88 pathway, efficiently eliminating invading ETECK88.

In mouse jejunum and ileum tissues, we showed that the administration of baclofen to activate GABA_BR notably reduced the mRNA levels of IL-1 β , IL-6, IL-17A, TNF- α , CXCL9, GMCSE, and MCP-1, while the expression of anti-inflammatory factors such as IL-4, IL-10, and TGF- β increased considerably. These data indicated that GABA_BR activation had a protective effect on mice infected with ETECK88. It has been reported that immune cells such as macrophages are excellent sources of inflammatory cytokines [61]. To date, macrophages are classified into two main functional types: classically activated (M1) macrophages and alternatively activated (M2) macrophages [62]. Commonly, M1 macrophages secrete a range of proinflammatory factors, such as IL-1 β , IL-6, and TNF- α , and enhance their specific markers CD16, CD32, CD80, CD86, MHCII, and iNOS. Conversely, the anti-inflammatory mediators IL-4, IL-10, and TGF- β are primarily expressed by M2 macrophages, which express the markers Arg-1, CD163, CD206, and Ym-1/2. In addition, our previous research verified that EGCs express immune markers, including CD16, CD32, CD80, CD86, MHC II, iNOS, Arg1 and CD206, and cytokines, such as IL-1 β , IL-6, CXCL10, IFN- γ , and TGF- β , to distinguish their specific phenotypes, namely, E1 and E2, in various states [34, 69]. Recently, receptors of GABA, including GABA_BR, were shown to be expressed in EGCs and cells of the immune system [34, 60]. Our data in jejunum

and ileum tissues revealed that activation of GABA_BR by baclofen significantly impeded the production of CD16, CD32, CD68, CD80, CD86, MHC II, and iNOS, while Arg1 and CD206 were highly expressed, suggesting that GABA_BR activation may simultaneously inhibit the macrophage M1- and EGC E1-like phenotype and promote the M2 and E2 phenotype following ETECK88 infection. Next, we found that elicitation of GABA_BR strongly reduced ETECK88 loads in the jejunum and ileum. Moreover, 16S rDNA sequencing revealed a reduced abundance of pathogenic bacteria and increased richness of probiotics, including *Lactobacillus*, in the ileum. These data suggest that GABA_BR activation is conserved in the mouse host defense against ETECK88 invasion. In accordance with the *in vitro* experiment, pretreatment of mice with baclofen strongly restrained the production of MyD88 and increased the expression of the autophagy-related molecules Beclin 1 and LC3. This finding provides more evidence that GABA_BR-mediated autophagy activation is frequently associated with MyD88 signaling. In the future, we will simultaneously assess multiple autophagy-related proteins, including ATG, LC3-I/II, and p62, to guarantee extensive and methodical experimental results. Although elevated numbers of EGCs were found in the myenteric plexus and intestinal mucosa of ETECK88-infected mice, GABA_BR activation markedly reversed these trends. One reason for this was that increased EGCs mainly exhibited proinflammatory phenotypes, while GABA_BR activation promoted these phenotypes to anti-inflammatory phenotypes, including functional antibacterial activity. The second reason could be attributed to the inhibitory effect of GABA_BR activation on cell transfer from the myenteric plexus to the mucous layer. However, we would like to stress some disadvantages presented in our current research. Due to technical limitations, it was difficult to determine the colocalization of ETECK88 and EGCs in the mouse jejunum and ileum, especially for bacteria-autophagosome combinations. Primary EGCs from intestinal tissues were separated and infected with ETECK88 directly to efficiently simulate *in vivo* conditions. More genes associated with autophagy, such as mTOR, p62, and ATG5, should be detected to further validate the role of GABA_BR. It has become apparent that we ought to have measured the protein levels of LC3-I/II rather than solely concentrating on mRNA levels, even though mRNA and protein expression levels are typically synchronized.

Conclusions

In conclusion, we highlighted a previously undiscovered role for GABA_BR in the regulation of the host defenses of EGCs against microbial invasion. ETECK88 significantly

inhibited autophagy, and its activation improved the inflammatory response and reduced the survival rate of patients infected with intracellular pathogens. Elicitation of GABA_BR strongly enhanced autophagy, thus increasing the bacteria-autophagosome combination to ultimately protect EGCs against ETECK88. In this molecular event, as an important factor, decreased levels of MyD88 strongly contributed to GABA_BR-mediated autophagy strengthening. Based on the findings of the present study, GABA_BR-mediated autophagy to enhance the antibacterial properties of EGCs may be beneficial for the development of therapeutic drugs for treating human and animal infective enteritis.

Materials and methods

Animals

C57BL/6 male mice aged 6–8 weeks with a wild-type (WT) background were purchased from Beijing Vital River Laboratory Animal Technology Co., Ltd., Beijing, China. Mice were maintained under specific pathogen-free conditions at a controlled temperature (20 °C ± 3 °C) and humidity (60% ± 5%), with free access to water and food. Our current study involving experimental mice was approved by the Committee for the Care and Use of Experimental Animals, China Agricultural University (No.: AW70604202-2-1). Great effort was made to attenuate pain and the number of animals.

Bacterial strains and cell line

The *Escherichia coli* K88 (ETECK88) strain with a WT background was obtained from Testobio Co., Ltd. (TS263632; Ningbo, China) to generate a strain with the mCherry gene, which is characterized by red fluorescence. These strains of bacteria were cultured in LB media at 37 °C. Cultures of bacteria were centrifuged at 3500 × g for 10 min, washed with sterile PBS, subjected to serial dilutions and plated on LB agar plates to count colony-forming units (CFU) for further experiments.

EGCs from the adult rat myenteric plexus were purchased from ATCC (CRL2690; VA, USA). EGCs were maintained in DMEM (AQ11995; Beijing Aoqing Biotechnology Co., Ltd., Beijing, China) supplemented with 10% heat-inactivated FBS (AQ-mv-09900; Beijing Aoqing Biotechnology Co., Ltd., Beijing, China), 2 mM glutamine (25030-081; Gibco, NY, USA), and penicillin–streptomycin solution (1X; BL505A; BioSharp, Hefei, China) at 37 °C with 5% CO₂.

Mouse infection

Mice were orally infected with 2 × 10⁹ CFU of ETECK88 or ETECK88-mCherry for 2 days and then killed after the indicated time [61]. For the activation of GABA_BR,

10 mg/kg of the GABA_BR agonist baclofen (HY-B0007; MCE, NJ, USA) was intraperitoneally injected into mice before and after ETEC infection [34]. Intestinal contents were collected to evaluate the richness of the microbiota, and intestinal tissues were fixed in 4% PFA. The other part of the tissue was stored at –80 °C for further testing. For measurement of the bacterial burdens, intestinal contents from ETECK88-mCherry-infected mice were collected and homogenized in sterile PBST, and serial dilutions of the homogenates were plated on LB agar plates, after which colonies were counted 24 h later.

EGC infection assay

EGCs were seeded into 6-well plates at 1 × 10⁶ cells per well and cultured for 24 h. The cells were inoculated with ETECK88 at a multiplicity of infection (MOI) of 5/10/20 for 3/6/12 h [59]. At this point, the GABA_BR agonist baclofen (10 μM; 1 h), the autophagy agonist RAPA (10/25 μM; 3/6/12 h; HY-10219; MCE, NJ, USA), or RAPA plus the autophagy inhibitor 3-MA (1/5/10 mM; 1 h; HY-19312; MCE, NJ, USA), CQ (10/25/50 μM; 1 h; HY-17589A; MCE, NJ, USA), or the MyD88 inhibitor TJ-M2010-5 (5/25 μM; 2 h; HY-139397; MCE, NJ, USA) were added where required before infection with or without ETEC.

Histology

For histopathology, intestinal tissue samples were fixed in 4% PFA and embedded in paraffin wax. Paraffin sections (5 μm) were then cut and stained with hematoxylin and eosin (H&E) and Alcian blue periodic acid Schiff (AB-PAS) to detect histological changes and mucus secretion, respectively. A 40× photographic microscope (Ni-U, Nikon, Tokyo, Japan) was used to image the whole intestinal cross-sections.

RNA isolation and quantitative real-time PCR (qRT–PCR)

Total RNA from intestinal tissues and EGCs was extracted with an Ultrapure RNA Kit (CW0597S; CWBIO, Beijing, China) following the manufacturer's instructions. One microgram of total RNA was reverse transcribed into complementary DNA using a SuperRT cDNA Synthesis Kit (CW0741; CWBIO, Beijing, China). cDNAs were mixed with primers and UltraSYBR Mixture (CW0957; CWBIO, Beijing, China) according to the manufacturer's protocols. The amplification steps were 95 °C for 10 min, followed by 40 cycles at 94 °C for 30 s, 60 °C for 30 s, and 72 °C for 30 s. Reactions were carried out on a CFX96 Real-Time Thermal Cycler (Bio-Rad, CA, USA). CT values were quantified using the 2^{–ΔΔCT} method, with GAPDH as the reference for normalization. The data are expressed as relative fold changes compared with those in the CON group. The sequences of the primers used in this study are listed in Supplementary Table 1 [34].

Western blotting (WB)

Intestinal tissues and cells were lysed in RIPA buffer (CW2333S; CWBIO, Beijing, China) supplemented with protease inhibitor cocktail (CW2200; CWBIO, Beijing, China). Total proteins were boiled in 1× SDS sample buffer (CW0027S; CWBIO, Beijing, China), separated by SDS-PAGE, and then transferred onto PVDF membranes (IPVH00010; Sigma, MO, USA). The membranes were blocked in 5% nonfat milk in PBST (E-1004; SLCY, Beijing, China) for 1.5 h at 37 °C and incubated with primary antibodies overnight at 4 °C. Then, appropriate secondary antibodies were incubated with the membranes for 1 h at 37 °C. β -actin was used for normalization of band intensities. Immunoreactivity band analysis was performed using an enhanced chemiluminescence (ECL) reagent (CW0049; CWBIO, Beijing, China), and bands were detected using a chemiluminescence system (5200; Tanon Science & Technology Co., Ltd., Shanghai, China). The primary antibodies used are listed in Supplementary Table 2.

Enzyme-linked immunosorbent assay (ELISA)

The concentrations of GABA_BR in intestinal tissues were determined by using commercial ELISA quantitative kits (JL51460-48T; J&L Biological, Shanghai, China) according to the manufacturer's protocol.

Immunofluorescence assays

Intestinal tissues were harvested, fecal pellets were flushed with PBS, and tissues were fixed with 4% PFA at 4 °C overnight. The MP was separated by stereomicroscopy (TP60; Beijing Tuopu Analytical Instruments Co., Ltd., Beijing, China). The tissues were permeabilized with 1% Triton X-100 at 37 °C for 2 h and then blocked with 5% donkey serum at 37 °C for 1 h. Double labeling was performed with goat anti-GFAP (1:1000; NB100-53809; Novus, CO, USA) and rabbit anti-S100 β (1:100; ab115803; Abcam, MA, USA) for 48 h at 4 °C. After incubation with primary antibodies, the samples were incubated for 24 h at 4 °C with biotin-SP (long spacer) affiniPure donkey anti-goat IgG (1:100; 705-065-147; Jackson, PA, USA). Then, the samples were incubated with AlexaFluor 594-conjugated streptavidin (1:200; S11227; Invitrogen, CA, USA) and AlexaFluor 488-conjugated antibody against rabbit IgG (1:100; A11034; Invitrogen, CA, USA) for 24 h at 4 °C. For mucosal layer single immunofluorescence, 40 μ m-thick tissue sections were processed and incubated with GFAP and S100 β and then loaded in biotin-SP (long spacer) affiniPure donkey anti-goat IgG and biotin-SP (long spacer) affiniPure donkey anti-rabbit IgG (1:100; 711-065-152; Jackson, PA, USA). Samples were subjected to Alexa Fluor 488-conjugated streptavidin (1:200; S11223; Invitrogen, CA, USA). Nuclei

were stained in the MP and tissue sections using DAPI (0100-20; SouthernBiotech, AL, USA). The negative control was subjected to the same procedure except that the primary antibodies were substituted with PBS. Labeled myenteric plexuses and tissue sections were visualized by a confocal laser-scanning microscope (TCSSP8; Leica, Wetzlar, Germany) to capture fluorescence images. Three slices were randomly selected for each group (five regions per slice, 6.25 μ m \times 6.25 μ m) to calculate the number of positive cells.

CFU Counting of Infected EGCs

To assess intracellular bacterial viability, the cells were infected with ETECK88 for 3 or 6 h. The cells were subsequently washed three times with PBS and cultured in DMEM supplemented with 50 μ g/mL gentamicin for 1 h to eliminate extracellular bacteria. Then, the medium was replaced with 0.2% Triton X-100 to release intracellular bacteria. Thereafter, bacteria were harvested and inoculated onto LB agar plates, and colonies were counted at 24 h [28].

Tandem pCMV-mCherry-GFP-LC3B transfection

EGCs were grown on 48-well plates until they reached 60%–70% confluence and then transfected with the pCMV-mCherry-GFP-LC3B plasmid using Lipo8000TM (C0533; Beyotime, Shanghai, China) for 24 h. After infection with the ETECK88 strain following the procedure, the cells were fixed with 4% PFA and imaged with a confocal laser-scanning microscope. The pCMV-mCherry-GFP-LC3B protein exhibited both red (mCherry) and green (GFP) fluorescence at neutral pH. The acidic environment of the lysosome causes quenching of the GFP signal, whereas the mCherry signal is more stable. Thus, the yellow (red + green) and red-only puncta represent the formation of autophagosomes and autolysosomes, respectively. The number of yellow and red dots per cell was counted under a confocal microscope (>20 cells/group).

Interactions between bacteria and autophagosomes

To assess the autophagic flux status in response to ETEC infection, a tandem pEGFP-LC3B plasmid was transfected into EGCs for 24 h. After infection with ETECK88-mCherry strains following the procedure, the cells were fixed with 4% PFA and imaged with a confocal laser-scanning microscope to visualize the combination of ETECK88-mCherry-autophagosomes.

Plasmid construction

The DNA fragment corresponding to the coding sequence of the MyD88 gene was amplified by PCR and subcloned and inserted into the pLV3-U6-MCS-shRNA-EF1a-CopGFP-Puro vector (P29436; Lanjiek Biotechnology

Co., Ltd., Haerbin, China) between the EcoRI and BamHI sites to construct the pLV3-U6-MyD88-shRNA CopGfp-Puro. The plasmid constructs were sequenced by Sangon Biotech Co., Ltd. (Shanghai, China) to verify 100% correspondence with the original sequence.

shRNA transduction

EGCs were seeded in 6-well culture dishes at a density of 3×10^5 cells/well. After incubation for 24 h, the cells were transfected with the pLV3-U6-MyD88-shRNA CopGfp-Puro plasmid using PEI transfection reagent (24765; Polysciences, PA, USA) according to the manufacturer's instructions. Gene silencing efficiency was examined by WB after 48 h of transfection.

16S rDNA amplicon sequencing of intestinal microbiota

The diversity of the intestinal microbiota was evaluated by Biomarker Technologies Co., Ltd., Beijing, China, using 16S rDNA amplicon sequencing according to a previously described method [62]. Content samples were freshly collected and stored at -80°C before use. DNA was extracted by the SDS method using universal primers to amplify the V3-V4 region of 16S rDNA. Then, the PCR products were evaluated on an Illumina HiSeq platform to evaluate the sequences and analyze the data.

Statistical analysis

Two-tailed unpaired t tests were used for comparisons of two groups. For comparisons of multiple groups, one-way ANOVA was applied, followed by Dunnett's multiple comparisons test. Before analysis, the normality of the distribution of all the data and the homogeneity of variance were checked. The data are shown as the mean \pm standard error of the mean (SEM). Differences were considered significant at * or # $p < 0.05$, ** or ## $p < 0.01$, *** or ### $p < 0.001$ (ns: not significant). All the statistical tests were carried out with GraphPad Prism 9 (GraphPad Software, SD, USA).

Supplementary Information

The online version contains supplementary material available at <https://doi.org/10.1186/s44280-024-00051-1>.

Supplementary Material 1.

Acknowledgments

Not applicable.

Authors' contributions

Z.D. and Y.M. conceived and designed the study. Z.D., J.L. and J.W. performed the experiments and collected all the data. Z.D. and L.W. conducted the statistical analyses. Z.D. and Y.M. drafted and revised the manuscript. Z.H. and Y.M. provided administrative, technical, and material support. All the authors have read and approved the final manuscript.

Funding

This work was financially supported by the National Natural Science Foundation of China (31772686), National Key R&D Program of China (2022YFD1801105) and Beijing Municipal Natural Science Foundation (6232021).

Availability of data and materials

All data that support the findings of this study are available from the corresponding author upon reasonable request.

Declarations

Ethics approval and consent to participate

All animal experiments were approved by the Committee for the Care and Use of Experimental Animals, China Agricultural University (No.: AW70604202-2-1).

Consent for publication

Not applicable.

Competing interests

The authors declare that they have no competing interests.

Received: 8 April 2024 Revised: 29 May 2024 Accepted: 29 May 2024

Published online: 14 June 2024

References

- Kiššová Z, Mudroňová D, Link R, Tkáčiková L. Immunomodulatory effect of probiotic exopolysaccharides in a porcine in vitro co-culture model mimicking the intestinal environment on ETEC infection. *Vet Res Commun.* 2024;48:705–24.
- De Lorimier AJ, Byrd W, Hall ER, Vaughan WM, Tang D, Roberts ZJ, et al. Murine antibody response to intranasally administered enterotoxigenic *Escherichia coli* colonization factor CS6. *Vaccine.* 2003;21:2548–55.
- Verecke N, Van Hoorde S, Sperling D, Theuns S, Devriendt B, Cox E. Virotyping and genetic antimicrobial susceptibility testing of porcine ETEC/STEC strains and associated plasmid types. *Front Microbiol.* 2023;14:1139312.
- Caruso R, Lo BC, Núñez G. Host–microbiota interactions in inflammatory bowel disease. *Nat Rev Immunol.* 2020;20:411–26.
- Gong L, Devenish RJ, Prescott M. Autophagy as a macrophage response to bacterial infection. *IUBMB Life.* 2012;64:740–7.
- Zhang C, Huang C, Xia H, Xu H, Tang Q, Bi F. Autophagic sequestration of SQSTM1 disrupts the aggresome formation of ubiquitinated proteins during proteasome inhibition. *Cell Death Dis.* 2022;13:615.
- Xia Y, Chen S, Zhao Y, Chen S, Huang R, Zhu G, et al. GABA attenuates ETEC-induced intestinal epithelial cell apoptosis involving GABA_AR signaling and the AMPK-autophagy pathway. *Food Funct.* 2019;10:7509–22.
- Soenen S, Rayner CK, Jones KL, Horowitz M. The aging gastrointestinal tract. *Curr Opin Clin Nutr Metab Care.* 2016;19:12–8.
- Bayrer JR, Castro J, Venkataraman A, Touhara KK, Rossen ND, Morrie RD, et al. Gut enterochromaffin cells drive visceral pain and anxiety. *Nature.* 2023;616:137–42.
- Cheng LK, O'Grady G, Du P, Egbuji JU, Windsor JA, Pullan AJ. Gastrointestinal system. *Wires Mech Dis.* 2010;2:65–79.
- Eckstein M-T, Moreno-Velásquez SD, Pérez JC. Gut bacteria shape intestinal microhabitats occupied by the fungus *Candida albicans*. *Curr Biol.* 2020;30:4799–4807.e4.
- Yan M, Su A, Pavasutthipaisit S, Spriewald R, Graßl GA, Beineke A, et al. Infection of porcine enteroids and 2D differentiated intestinal epithelial cells with rotavirus A to study cell tropism and polarized immune response. *EMI.* 2023;12:2239937.
- Furness JB. The enteric nervous system and neurogastroenterology. *Nat Rev Gastroenterol Hepatol.* 2012;9:286–94.
- Cameron O, Neves JF, Gentleman E. Listen to your gut: key concepts for bioengineering advanced models of the intestine. *Adv Sci.* 2024;11:2302165.

15. Dershowitz LB, Li L, Pasca AM, Kaltschmidt JA. Anatomical and functional maturation of the mid-gestation human enteric nervous system. *Nat Commun.* 2023;14:2680.
16. Seguela L, Gulbransen BD. Enteric glial biology, intercellular signaling and roles in gastrointestinal disease. *Nat Rev Gastroenterol Hepatol.* 2021;18:571–87.
17. Laddach A, Chng SH, Lasrado R, Prokatzky F, Shapiro M, Erickson A, et al. A branching model of lineage differentiation underpinning the neurogenic potential of enteric glia. *Nat Commun.* 2023;14:5904.
18. Morales-Soto W, Gonzales J, Jackson WF, Gulbransen BD. Enteric glia promote visceral hypersensitivity during inflammation through intercellular signaling with gut nociceptors. *Sci Signal.* 2023;16:eadg1668.
19. Selgrad M, De Giorgio R, Fini L, Cogliandro RF, Williams S, Stanghellini V, et al. JC virus infects the enteric glia of patients with chronic idiopathic intestinal pseudo-obstruction. *Gut.* 2009;58:25–32.
20. Chow AK, Grubišić V, Gulbransen BD. Enteric glia regulate lymphocyte activation via autophagy-mediated MHC-II expression. *Cell Mol Gastroenterol.* 2021;12:1215–37.
21. Flamant M, Aubert P, Rolli-Derkinderen M, Bourreille A, Neunlist MR, Mahe MM, et al. Enteric glia protect against *Shigella flexneri* invasion in intestinal epithelial cells: a role for S-nitrosoglutathione. *Gut.* 2011;60:47–84.
22. Krantis A. GABA in the mammalian enteric nervous system. *Physiology.* 2000;15:284–90.
23. Lake JJ, Heuckeroth RO. Enteric nervous system development: migration, differentiation, and disease. *Am J Physiol Gastrointest Liver Physiol.* 2013;305:G1–G24.
24. Seif M, Brown JF, Mills J, Bhandari P, Belelli D, Lambert JJ, et al. Molecular and functional diversity of GABA-A receptors in the enteric nervous system of the mouse colon. *J Neurosci.* 2014;34:10361–78.
25. Auteri M, Zizzo MG, Serio R. GABA and GABA receptors in the gastrointestinal tract: from motility to inflammation. *Pharmacol Res.* 2015;93:11–21.
26. An J, Seok H, Ha E-M. GABA-producing *Lactobacillus plantarum* inhibits metastatic properties and induces apoptosis of 5-FU-resistant colorectal cancer cells via GABAB receptor signaling. *J Microbiol.* 2021;59:202–16.
27. Ma X, Sun Q, Sun X, Chen D, Wei C, Yu X, et al. Activation of GABAA Receptors in colon epithelium exacerbates acute colitis. *Front Immunol.* 2018;9:987.
28. Kim JK, Kim YS, Lee H-M, Jin HS, Neupane C, Kim S, et al. GABAergic signaling linked to autophagy enhances host protection against intracellular bacterial infections. *Nat Commun.* 2018;9:4184.
29. Sanders RD, Grover V, Goulding J, Godlee A, Gurney S, Snelgrove R, et al. Immune cell expression of GABAA receptors and the effects of diazepam on influenza infection. *J Neuroimmunol.* 2015;282:97–103.
30. Kasaragod VB, Mortensen M, Hardwick SW, Wahid AA, Dorovych V, Chirgadze DY, et al. Mechanisms of inhibition and activation of extrasynaptic $\alpha\beta$ GABAA receptors. *Nature.* 2022;602:529–33.
31. Wang H, Zhang H, Sun Z, Chen W, Miao C. GABAB receptor inhibits tumor progression and epithelial–mesenchymal transition via the regulation of Hippo/YAP1 pathway in colorectal cancer. *Int J Biol Sci.* 2021;17:1953–62.
32. Shu Q, Liu J, Liu X, Zhao S, Li H, Tan Y, et al. GABA_BR/GSK-3 β /NF- κ B signaling pathway regulates the proliferation of colorectal cancer cells. *Cancer Med.* 2016;5:1259–67.
33. Ge P, Lei Z, Yu Y, Lu Z, Qiang L, Chai Q, et al. *tuberculosis* PknG manipulates host autophagy flux to promote pathogen intracellular survival. *Autophagy.* 2022;18:576–94.
34. Deng Z, Li D, Yan X, Lan J, Han D, Fan K, et al. Activation of GABA receptor attenuates intestinal inflammation by modulating enteric glial cells function through inhibiting NF- κ B pathway. *Life Sci.* 2023;329:121984.
35. Teymournejad O, Sharma AK, Abdelwahed M, Kader M, Ahmed I, Elkafas H, et al. Hepatocyte-specific regulation of autophagy and inflammasome activation via MyD88 during lethal *Ehrlichia* infection. *Front Immunol.* 2023;14:1212167.
36. Tilstra JS, Kim M, Gordon RA, Leibler C, Cosgrove HA, Bastacky S, et al. B-cell–intrinsic Myd88 regulates disease progression in murine lupus. *J Exp Med.* 2023;220:e20230263.
37. Qi M, Liao S, Wang J, Deng Y, Zha A, Shao Y, et al. MyD88 deficiency ameliorates weight loss caused by intestinal oxidative injury in an autophagy-dependent mechanism. *J Cachexia Sarcopenia Muscle.* 2022;13:677–95.
38. Zandieh Z, Govahi A, Aghamajidi A, Raoufi E, Amjadi F, Aghajanzour S, et al. TLR-1, TLR-2, and TLR-6 MYD88–dependent signaling pathway: a potential factor in the interaction of high-DNA fragmentation human sperm with fallopian tube epithelial cells. *Clin Exp Reprod Med.* 2023;50:44–52.
39. Bayer AL, Smolgovsky S, Ngwenyama N, Hernández-Martínez A, Kaur K, Sulka K, et al. T-Cell MyD88 Is a Novel Regulator of Cardiac Fibrosis Through Modulation of T-Cell Activation. *Circ Res.* 2023;133:412–29.
40. Yoshitaka T, Mukai T, Kittaka M, Alford LM, Masrani S, Ishida S, et al. Enhanced TLR-MYD88 Signaling Stimulates Autoinflammation in SH3BP2 Cherubism Mice and Defines the Etiology of Cherubism. *Cell Rep.* 2014;8:1752–66.
41. Luis AS, Hansson GC. Intestinal mucus and their glycans: A habitat for thriving microbiota. *Cell Host & Microbe.* 2023;31:1087–100.
42. Shi Y, Li S, Zhang H, Zhu J, Che T, Yan B, et al. The effect of macrophage polarization on the expression of the oxytocin signaling system in enteric neurons. *J Neuroinflammation.* 2021;18:261.
43. Von Mentzer A, Svennerholm A-M. Colonization factors of human and animal-specific enterotoxigenic *Escherichia coli* (ETEC). *Trends Microbiol.* 2023;32:448–64.
44. Fleckenstein JM, Hardwidge PR, Munson GP, Rasko DA, Sommerfelt H, Steinsland H. Molecular mechanisms of enterotoxigenic *Escherichia coli* infection. *Microbes Infect.* 2010;12:89–98.
45. Kawabata S, Boyaka PN, Coste M, Fujihashi K, Yamamoto M, McGhee JR, et al. Intraepithelial lymphocytes from villus tip and crypt portions of the murine small intestine show distinct characteristics. *Gastroenterology.* 1998;115:866–73.
46. Luo P, Liu D, Li C, He WX, Zhang CL, Chang MJ. Enteric glial cell activation protects enteric neurons from damage due to diabetes in part via the promotion of neurotrophic factor release. *Neurogastroenterol Motil.* 2018;30:e13368.
47. Cirillo C, Sarnelli G, Esposito G, Grosso M, Petruzzelli R, Izzo P, et al. Increased mucosal nitric oxide production in ulcerative colitis is mediated in part by the enteroglia-derived S100B protein. *Neurogastroenterol Motil.* 2009;21:1209.
48. Cirillo C, Sarnelli G, Turco F, Mango A, Grosso M, Aprea G, et al. Pro-inflammatory stimuli activates human-derived enteroglia cells and induces autocrine nitric oxide production. *Neurogastroenterol Motil.* 2011;23:e372–82.
49. Hollifield IE, Motyka NI, Fernando KA, Bitoun JP. Heat-labile enterotoxin decreases macrophage phagocytosis of enterotoxigenic *Escherichia coli*. *Microorganisms.* 2023;11:2121.
50. Zhang L, Yu S, Ning X, Fang H, Li J, Zhi F, et al. A LysR transcriptional regulator manipulates macrophage autophagy flux during *Brucella* infection. *Front Cell Infect Microbiol.* 2022;12:858173.
51. Pankiv S, Clausen TH, Lamark T, Brech A, Bruun J-A, Outzen H, et al. p62/SQSTM1 binds directly to Atg8/LC3 to facilitate degradation of ubiquitinated protein aggregates by autophagy. *J Biol Chem.* 2007;282:24131–45.
52. Bjørkøy G, Lamark T, Brech A, Outzen H, Perander M, Øvervatn A, et al. p62/SQSTM1 forms protein aggregates degraded by autophagy and has a protective effect on huntingtin-induced cell death. *J Cell Biol.* 2005;171:603–14.
53. Zeng X, Niu Y, Qin G, Zhang D, Chen L. Dysfunction of inhibitory interneurons contributes to synaptic plasticity via GABABR-pNDR2B signaling in a chronic migraine rat model. *Front Mol Neurosci.* 2023;16:1142072.
54. Jiang S, He M, Xiao L, Sun Y, Ding J, Li W, et al. Prenatal GABAB receptor agonist administration corrects the inheritance of autism-like core behaviors in offspring of mice prenatally exposed to valproic acid. *Front Psychiatry.* 2022;13:835993.
55. Sun X, Lin M, Tian Z, Ma Y, Lv L. GABA/baclofen stabilizes PD-L1 and enhances immunotherapy of breast cancer. *Heliyon.* 2024;10:e28600.
56. Zeng X, Niu Y, Qin G, Zhang D, Zhou J, Chen L. Deficiency in the function of inhibitory interneurons contributes to glutamate-associated central sensitization through GABABR2-SynCAM1 signaling in chronic migraine rats. *FASEB J.* 2020;34:14780–98.
57. Tran G-B, Ding J, Ye B, Liu M, Yu Y, Zha Y, et al. Caffeine supplementation and FOXM1 inhibition enhance the antitumor effect of statins in neuroblastoma. *Cancer Res.* 2023;83:2248–61.
58. Gao J, Gao Y, Lin S, Zou X, Zhu Y, Chen X, et al. Effects of activating GABAB1 receptor on proliferation, migration, invasion and epithelial–mesenchymal transition of ovarian cancer cells. *J Ovarian Res.* 2020;13:126.

59. Turco F, Sarnelli G, Cirillo C, Palumbo I, De Giorgi F, D'Alessandro A, et al. Enteroglia-derived S100B protein integrates bacterium-induced Toll-like receptor signaling in human enteric glial cells. *Gut*. 2014;63:105–15.
60. Chen Y, Cao B, Zheng W, Xu T. ACKR4a induces autophagy to block NF- κ B signaling and apoptosis to facilitate *Vibrio harveyi* infection. *iScience*. 2023;26:106105.
61. Chu Q, Sun Y, Cui J, Xu T. MicroRNA-3570 modulates the NF- κ B pathway in teleost fish by targeting MyD88. *J Immunol*. 2017;198:3274–82.
62. Kader M, Alaoui-EL-Azher M, Vorhauer J, Kode BB, Wells JZ, Stolz D, et al. MyD88-dependent inflammasome activation and autophagy inhibition contributes to Ehrlichia-induced liver injury and toxic shock. *PLoS Pathog*. 2017;13:e1006644.
63. Takeuchi O, Hoshino K, Akira S. Cutting edge: TLR2-deficient and MyD88-deficient mice are highly susceptible to *Staphylococcus aureus* infection. *J Immunol*. 2000;165:5392–6.
64. Funes SC, Rios M, Escobar-Vera J, Kalergis AM. Implications of macrophage polarization in autoimmunity. *Immunology*. 2018;154:186–95.
65. Louiselle AE, Niemiec SM, Zgheib C, Liechty KW. Macrophage polarization and diabetic wound healing. *Transl Res*. 2021;236:109–16.
66. Da Silveira Barcelos Morais A, De Oliveira EC, Neto SG, Luquetti AO, Toshio Fujiwara R, Correa Oliveira R, et al. Enteroglia cells act as antigen-presenting cells in chagasic megacolon. *Human Pathol*. 2011;42:522–32.
67. Jin Z, Mendu SK, Birnir B. GABA is an effective immunomodulatory molecule. *Amino Acids*. 2013;45:87–94.
68. Ren W, Yin J, Xiao H, Chen S, Liu G, Tan B, et al. Intestinal microbiota-derived GABA mediates interleukin-17 expression during enterotoxigenic *Escherichia coli* infection. *Front Immunol*. 2017;7:685.
69. Li H, Shang Z, Liu X, Qiao Y, Wang K, Qiao J. *Clostridium butyricum* alleviates enterotoxigenic *Escherichia coli* K88-induced oxidative damage through regulating the p62-Keap1-Nrf2 signaling pathway and remodeling the cecal microbial community. *Front Immunol*. 2021;12:771826.

Publisher's Note

Springer Nature remains neutral with regard to jurisdictional claims in published maps and institutional affiliations.